RSC Advances

PAPER

View Article Online
View Journal | View Issue

Cite this: *RSC Adv.*, 2014, **4**, 54158

Synthesis and phase behavior of mesogen-jacketed liquid crystalline polymer with triphenylene discotic liquid crystal mesogen unit in side chains

Jianfeng Ban, Sheng Chen and Hailiang Zhang*

Received 30th July 2014
Accepted 22nd September 2014

DOI: 10.1039/c4ra07824a

www.rsc.org/advances

A novel mesogen-jacketed liquid crystalline polymer (MJLCP) containing two triphenylene (Tp) units in the side chains, named poly[bis(3,6,7,10,11-pentakis(hexyloxy)triphenylen-2-yl)2-vinyl terephthalate] (PBTCS), was designed and successfully synthesized *via* conventional free radical polymerization. The chemical structure of the monomer was confirmed by $^{1}H/^{13}C$ NMR and high-resolution mass spectrometry. The molecular characterization of the polymer was performed with ^{1}H NMR, gel permeation chromatography (GPC) and thermogravimetric analysis (TGA). The phase structure and transition of the polymer were investigated by the combination of techniques, including differential scanning calorimetry (DSC), polarizing optical microscope (POM), 1D/2D wide-angle X-ray diffraction (1D and 2D WAXD) and 1D small-angle X-ray scattering (1D SAXS). The results showed that the PBTCS reached a relatively high glass transition temperature and formed a higher symmetry hexagonal columnar (Φ_H) phase due to the strong coupling effect between the Tp moieties and the MJLCP main chain.

Introduction

Polymeric discotic liquid crystals (DLCs) have attracted considerable attention because of their capability of self-assembling into different well-ordered structures, which produce interesting physical properties that can be applied in devices such as optical compensation films, one-dimensional conductors, anisotropic photoconductors, and photovoltaic solar cells.[1–15] DLCs were first realized by Ringsdorf *et al.*[16] and subsequently many types of discotic polymers have been prepared. Among them, the phase behavior and phase structure of end-on side-chain liquid crystal polymers (SCLCPs) containing triphenylene (Tp) derivatives with long flexible spacer as linkers have been widely investigated.[15,17–20] The research shows that this kind of SCLCPs can self-organize into well-ordered, self-healable supramolecular columns due to the π–π stacking of the planar aromatic cores and the van der Waals interactions of the peripheral chains, for example, poly(meth) acrylates, polysiloxanes and polyacetylenes containing Tp moieties in the side chains.[21–27]

Mesogen-jacketed liquid crystalline polymers (MJLCPs) have been systematically studied during the past two decades because they display many special properties, similar to the rigid backbone polymers, such as high glass transition temperature, broad temperature range of mesophase, long persistence length in good solvent, and forming a banded texture after mechanical shearing in the LC state.[28–35] MJLCPs are side-on side-chain liquid crystalline polymers, in which the bulky side-chain mesogens are side-on attached to the flexible main chain through a short spacer or a covalent bond. Owing to the strong steric effect, many MJLCPs show columnar phases, in which each cylinder is formed by a single MJLCP chain molecule. Recently, a series of MJLCPs containing two triphenylene (Tp) units with different lengths of the methylene units between the terephthalate core and Tp moieties in the side chains have been prepared by Zhu *et al.* and the phase behaviors of these combined main-chain/side-chain liquid-crystalline (LC) polymers were investigated.[36,37] The results indicated that the individual ordered structures developed at different temperatures by these two LC building blocks were not only competitive but also promotive to each other.

An interesting point arises concerning the properties of MJLCPs when the Tp moieties are directly connected to the main chain. Our main concern is whether the "jacketed-effect" influences the π–π stacking of the Tp mesogen. Therefore, in this work, we design and synthesize a novel MJLCP with Tp DLCs as the mesogens unit that is directly connected to the repeating unit of the poly(vinyl terephthalate) main chain without a flexible spacer. The target polymer PBTCS is shown in Chart 1. In this work, the phase transitions and structures of PBTCS have been studied in detail. To the best of our knowledge, this is the first report of MJLCP with discotic mesogens directly connected to the main chain without a flexible spacer. The polymer exhibiting extraordinary stabilized hexagonal columnar structures could guide the design of ordered functional LC polymers bearing discotic mesogens.

Key Laboratory of Polymeric Materials and Application Technology of Hunan Province, Key Laboratory of Advanced Functional Polymer Materials of Colleges, Universities of Hunan Province, College of Chemistry, Xiangtan University, Xiangtan 411105, Hunan Province, China. E-mail: huaxuechensheng@163.com; zhl1965@xtu.edu.cn

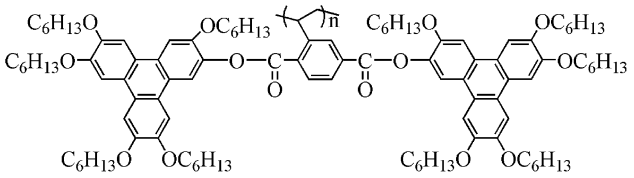

Chart 1 Chemical structure of PBTCS.

Experimental

Materials

The precursor 2-vinyl terephthalic acid (VTA) was synthesized according to previous work.[38] Anhydrous tetrahydrofuran (THF) was distilled from sodium benzophenone ketyl under argon and used immediately. 2,2-Azobisisobutyronitrile (AIBN) was freshly recrystallized from methanol. Dichloromethane (CH_2Cl_2) was dried over anhydrous magnesium sulfate. All other reagents and solvents were used as received without further purification.

Instruments and measurements

Nuclear magnetic resonance (NMR). $^1H/^{13}C$ NMR measurements were performed using a Bruker ARX400 MHz spectrometer using with $CDCl_3$ as solvent, with tetramethylsilane (TMS) as the internal standard at ambient temperature. The chemical shifts were reported using the ppm scale.

Gel permeation chromatography (GPC). The apparent number average molecular weight (M_n) and polydispersity index (PDI = M_w/M_n) were measured using a GPC (Waters 1515) instrument with a set of HT3, HT4 and HT5 columns. The μ-Styragel columns used THF as an eluent and the flow rate was 1.0 mL min^{-1} at 38 °C. The GPC data were calibrated with polystyrene standards.

Thermogravimetric analysis (TGA). TGA was performed using a TA SDT 2960 instrument at a heating rate of 20 °C min^{-1} in a nitrogen atmosphere.

Differential scanning calorimetry (DSC). DSC traces of the polymer were obtained using a TA Q10 DSC instrument. The temperature and heat flow were calibrated using standard materials (indium and zinc) at cooling and heating rates of 10 °C min^{-1}. The sample with a typical mass of about 5 mg was encapsulated in sealed aluminum pans.

Polarizing optical microscope (POM). LC texture of the polymer was examined under POM (Leica DM-LM-P) equipped with a Mettler Toledo hot stage (FP82HT).

One-dimensional wide-angle X-ray diffraction (1D WAXD). 1D WAXD experiments were performed using a Bruker AXS D8 Advance diffractometer with a 40 kV FL tubes as the X-ray source (Cu Kα) and a LYNXEYE_XE detector. Background scattering was recorded and subtracted from the sample patterns. The heating and cooling rates in the 1D WAXD experiments were 10 °C min^{-1}.

Two-dimensional wide-angle X-ray diffraction (2D WAXD). 2D WAXD was carried out using a Bruker AXS D8 Discover diffractometer with a 40 kV FL tubes as the X-ray source (Cu Kα) and the VANTEC 500 detector. The point-focused X-ray beam was aligned either perpendicular or parallel to the mechanical shearing direction. For both the 1D and 2D WAXD experiments, the background scattering was recorded and subtracted from the sample patterns.

1D small-angle X-ray scattering (1D SAXS). 1D SAXS experiments were performed using a high flux SAXS instrument (SAXSess, Anton Paar) equipped with the Kratky block collimation system and a Philips PW3830 sealed tube X-ray generator (Cu Kr).

Synthesis of monomer

The chemical structures and synthetic procedures for the monomer (MBTC) are shown in Scheme 1. 2-Hydroxyl-3,6,7,10,11-pentakis(hexyloxy)triphenylene (PHT) was easy to

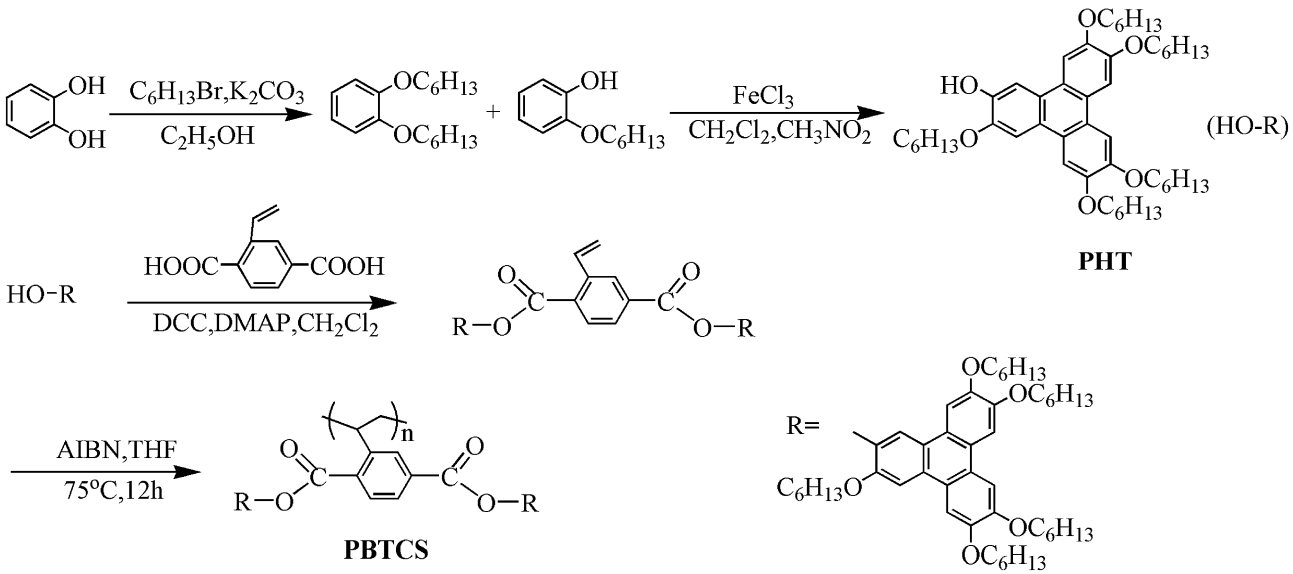

Scheme 1 Synthetic route of the polymer (PBTCS).

obtain as mentioned in our previous work. The experimental details are described as follows: 2-hydroxyl-3,6,7,10,11-pentakis (hexyloxy)triphenylene (PHT) and 2-vinyl terephthalic acid (VTA), were facilely synthesized *via* DCC condensation. PHT (3.875 g, 5.2 mmol), VTA (0.5 g, 2.6 mmol), *N*,*N*′-dicyclohexylcarbodiimide (DCC, 1.073 g, 5.2 mmol), 4-(dimethylamino) pyridine (DMAP, 0.06 g, 0.52 mmol), and dried CH_2Cl_2 (100 mL) were mixed in a 250 mL round-bottomed flask and then stirred at ambient temperature for 24 h. The floating solid was filtered, and the solvent was evaporated under reduced pressure. The crude product was purified using silica gel column chromatography with CH_2Cl_2 as eluent and subsequent recrystallization from methyl alcohol and it was obtained as a faint yellow powder. Yield: 48%. ^{1}H NMR (δ): 8.62 (d 1H, Ar–*H*), 8.37–8.35 (e 2H, Ar–*H*), 8.26–7.90 (f 2H, Ar–*H*, l 2H, Ar–*H*, m 4H, Ar–*H*, n 4H, Ar–*H*), 7.85–7.82 (c 1H, –C*H*═), 5.98–5.93 (b 1H, ═CH_2), 5.54–5.51 (a 1H, ═CH_2), 4.24 (g 20H, –CH_2–), 1.95 (h 20H, –CH_2–), 1.81 (i 20H, –CH_2–), 1.58 (j 40H, –CH_2–), 0.94 (k 30H, –CH_3). 13C NMR(δ): 14.06 (–*C*H_3), 22.54–31.73 (–*C*H_2–), 68.89 (–O*C*H_2–), 115.08 (═*C*H_2), 123.02 (aromatic *C*–O), 123.22–124.76 (aromatic *C*), 128.20 (middle aromatic *C*), 132.71 (–H*C*═*C*H_2), 139.72 (aromatic *C*–H*C*═*C*H_2), 148.86–149.85 (aromatic *C*–O), 158.08 (aromatic *C*–O), 164.33 (*C*═O). Mass spectrometry (MS) (*m*/*z*) [M] calcd for $C_{106}H_{148}O_{14}$, 1645.09; found, 1645 + 1.

Synthesis of polymer

As shown in Scheme 1, the polymer was synthesized by conventional solution free-radical polymerization. The detailed procedure was carried out as follows: 0.3 g (0.18 mmol) of MBTC, 100 μL of tetrahydrofuran (THF) solution of 0.01 mmol AIBN, 2 mL of THF, and a magnetic stir bar were added into a polymerization tube; the tube was purged with nitrogen and subjected to three freeze–thaw cycles to remove any dissolved oxygen and sealed off under vacuum. Polymerization was performed at 75 °C for 12 h. Subsequently, the polymerization was stopped by dipping the tube in ice water. Then the tube was opened, and the reaction mixture was diluted with 10 mL of THF. The resultant polymer was precipitated and washed with methanol. To eliminate the unreacted monomers completely, the purification was repeated three times, until no peak was observed at the elution time of the monomer in gel permeation chromatography (GPC) measurement. The target polymer poly [bis(3,6,7,10,11-pentakis(hexyloxy)triphenylen-2-yl)2-vinyl terephthalate] (PBTCS) was obtained as a faint yellow solid. Yield: 68%.

Results and discussion

Synthesis and characterization of monomer and polymer

PHT was reacted with VTA *via* Steglich esterification to obtain the monomer. The monomer could be easily polymerized *via* free radical polymerization. The molecular characterizations of the polymer were summarized in Table 1. GPC analysis of the polymer shows that a number-average weight (M_n) of the PBTCS is 1.7×10^4 g mol^{-1}, with polydispersities of 1.43, confirming good polymerizability of the monomer. The chemical structure of the monomer was confirmed by ^{1}H/^{13}C NMR and high-resolution mass spectrometry. Fig. 1a and b shows the ^{1}H NMR spectra ($CDCl_3$) of the monomer MBTC and the polymer PBTCS, respectively. The characteristic resonance peaks of the vinyl group appearing at 5.54–5.93 and 7.82–7.85 ppm completely disappear after polymerization, and the resonance peaks of PBTCS were rather broad and consistent with the expected polymer structure, indicating successful polymerization as well.

Mesomorphic properties of the monomer

The phase behaviors of the monomer were examined by conventional analyses, including DSC and POM. In order to avoid thermal polymerization, the detection temperature of DSC and POM was below 210 °C. The thermograms of MBTC on both first cooling scans and the second heating scans were shown in Fig. 2, and its phase transition temperatures were collected in Table 2. The results showed that the MBTC presented crystal phase in low temperature (Fig. 3a) and formed columnar phase when the temperature was raised to 131 °C (Fig. 3b). With the increase in temperature, it turned into nematic phase (Fig. 3c). Once the temperature reached 204 °C, the schlieren textures disappeared, indicating entry into isotropic state, which was consistent with the DSC results.

The phase transitions and structure of the MBTC were further varied using the 1D WAXD instrument. Fig. 4 illustrates the 1D WAXD patterns of the MBTC obtained during the first heating process. As shown in Fig. 4, MBTC formed the crystal structure when the temperature was below 140 °C. With the increase in temperature, many diffraction peaks disappeared in the high 2θ range; moreover, the π–π interactions of the triphenylene were observed at ~25 °C, indicating that MBTC entered into the column structure. However, when the temperature was raised to 180 °C, the π–π interactions of the triphenylene disappeared in the high 2θ range, suggesting the formation of another ordered structure. Combining the POM

Table 1 Molecular characteristics of PBTCS

Polymer	M_n[a] ($\times 10^{-4}$ g mol^{-1})	PDI[a]	T_g[b] (°C)	T_g[c] (°C)	T_i[d] (°C)	T_d[e] (N_2)
PBTCS	1.7	1.43	217	222	285	385

[a] Determined by GPC in THF using PS standards. [b] Evaluated by DSC during the first cooling process at a rate of 10 °C min^{-1}, under a nitrogen atmosphere. [c] Evaluated by DSC during the second heating process at a rate of 10 °C min^{-1}, under a nitrogen atmosphere. [d] The phase transition temperature form liquid crystalline to isotropic phase (T_i) was evaluated by POM at a heating rate of 5 °C min^{-1}. [e] The temperatures at which 5% weight loss of the sample under a nitrogen [$T_d(N_2)$] was measured by TGA heating experiments at a rate of 20 °C min^{-1}.

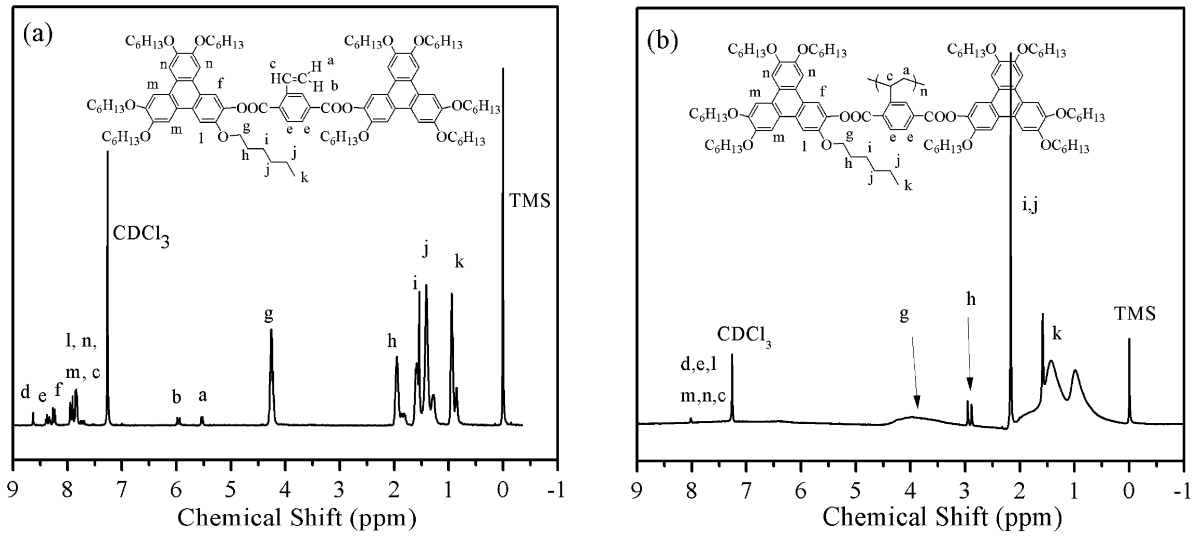

Fig. 1 ^{1}H NMR spectra of the monomer MBTC (a) and the polymer PBTCS (b) in $CDCl_3$.

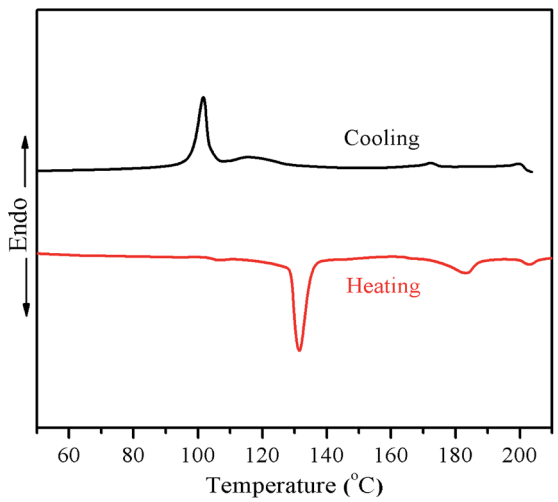

Fig. 2 DSC thermogram of MBTC during the first cooling and second heating at a rate of 5 °C min^{-1} under a nitrogen atmosphere.

Table 2 Liquid-crystalline properties of the monomer[a]

	Phase transitions (°C)	
Monomer	First cooling	Second heating
MBTC	I(201)N(172)Col(106)Cr	Cr(131)Col(178)N(204)I

[a] Cr: crystalline; N: nematic; Col: columnar; and I: isotropic phase.

result (as shown in Fig. 3c), the monomer exhibited the nematic phase at high temperature. At last, the diffusion peaks were observed in the low and high 2θ range, showing the isotropic phase.

Thermal and liquid crystalline properties of the polymer

The thermal and liquid crystalline properties of the polymer were investigated by TGA, DSC and POM. As shown in Table 1, the polymer exhibit excellent thermal stability, that is, the temperature (T_d) at 5% weight loss of the sample under nitrogen was 385 °C measured by TGA at a rate of 20 °C min^{-1}.

The phase transition behaviors of the polymer were investigated by DSC. Fig. 5 shows the first cooling and the second heating DSC curves of PBTCS at a rate of 10 °C min^{-1} under a nitrogen atmosphere after eliminating the thermal history. As can be noticed, the glass transition temperature (T_g) of the polymer can be observed. As expected, the polymer reached a relatively higher T_g (222 °C) compared to PP*n*V (*n* is the number of methylene units between the terephthalate core and Tp moieties in the side chains). For example, when $n = 3$, 6, 9, the T_g of the polymers was 60 °C, 21 °C and 6 °C, respectively, indicating that the T_g decreased with the increase of the spacer.[36,37] The DSC profile of PBTCS from 50 to 250 °C shows only a glass transition step but no endothermic peak correlating to a phase transition, which is characteristic for most MJLCPs reported. Due to the insensitivity of the DSC method to determine the phase transitions of the polymer except for glass transitions, POM and WAXD techniques were utilized to further investigate PBTCS LC phase behavior.

Birefringence of the polymer was observed by POM. The sample was cast from CH_2Cl_2 solution and slowly dried at room temperature, then slowly heated. The POM results are shown in Fig. 6. As can be seen from the figure, the pseudo focal-conic fan textures were observed at 213 °C, which is the typical texture of a columnar phase. When temperature reached 285 °C, the birefringence disappeared and the field of vision became dark, indicating that the polymer entered into the isotropic state. When cooled to room temperature from 285 °C, the birefringence was observed again, which implied the formation of ordered structure was reversible.

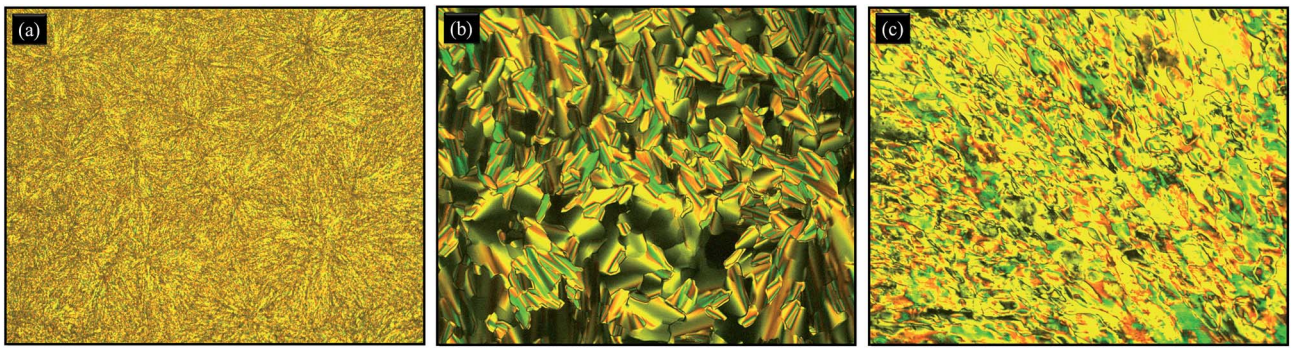

Fig. 3 The representative POM images of the texture of MBTC maintained at (a) 68 °C, (b) 160 °C and (c) 190 °C (200×).

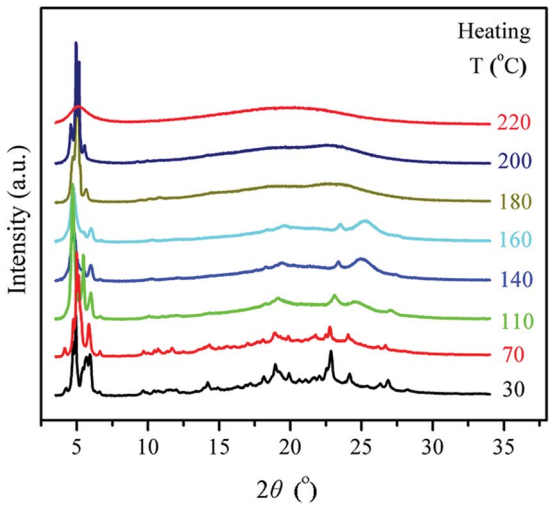

Fig. 4 1D WAXD patterns of MBTC during the first heating.

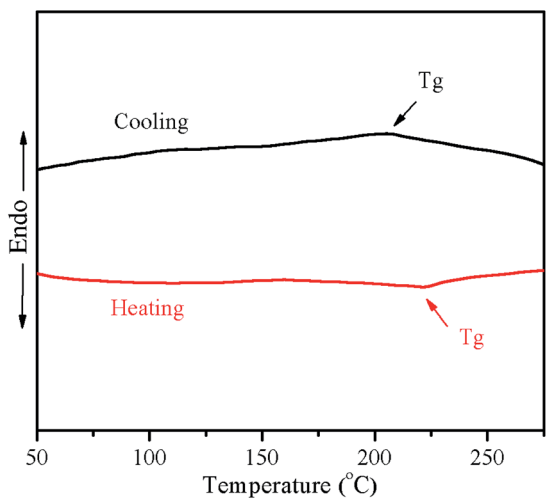

Fig. 5 DSC thermogram of PBTCS during the first cooling and second heating at a rate of 10 °C min^{-1} under a nitrogen atmosphere.

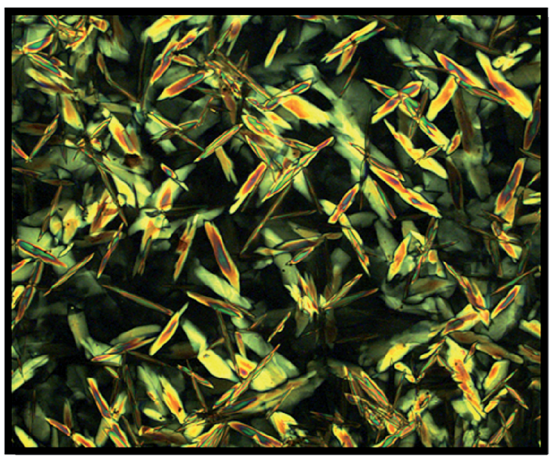

Fig. 6 The representative polarized micrograph of the texture at 213 °C of PBTCS (200×).

Phase structure identification of the polymer

To identify the phase structures of PBTCS, 1D (at different temperatures) and 2D WAXD experiments were carried out. For 1D WAXD experiments, a sample of about 50 mg of the polymer was added into an aluminum foil substrate. 2D WAXD pattern was recorded with the X-ray incident beam perpendicular to the shear direction. The sample was thermally annealed overnight at an appropriate temperature above T_g before performing 2D WAXD experiments.

1D WAXD profiles of PBTCS during the first heating and subsequent cooling processes are shown in Fig. 7a and b, respectively. Whether the temperature was lower or higher than the T_g of the polymer (222 °C), the patterns of the low-angle region renders two sharp diffraction peaks, indicating the existence of an ordered structure. With heating to higher temperatures, in the low-angle region the peaks slightly shifted to a lower angle and the first peak intensity increased due to thermal expansion. Two sharp peaks with a scattering vector ratio of $1 : 3^{1/2}$ ($q = 4\pi \sin\theta/\lambda$, where λ is the X-ray wavelength and 2θ is the scattering angle) appear, and the corresponding d-spacing values of the two peaks are 2.74 and 1.64 nm, which are indexed as the (100) and (110) diffractions, demonstrating an ordered hexagonal lattice with $a = b = 3.17$ nm, $\gamma = 120°$. The absence of (hkl) diffractions indicates that the polymers formed a 2D positional order, similar to many other MJLCPs.[39,40]

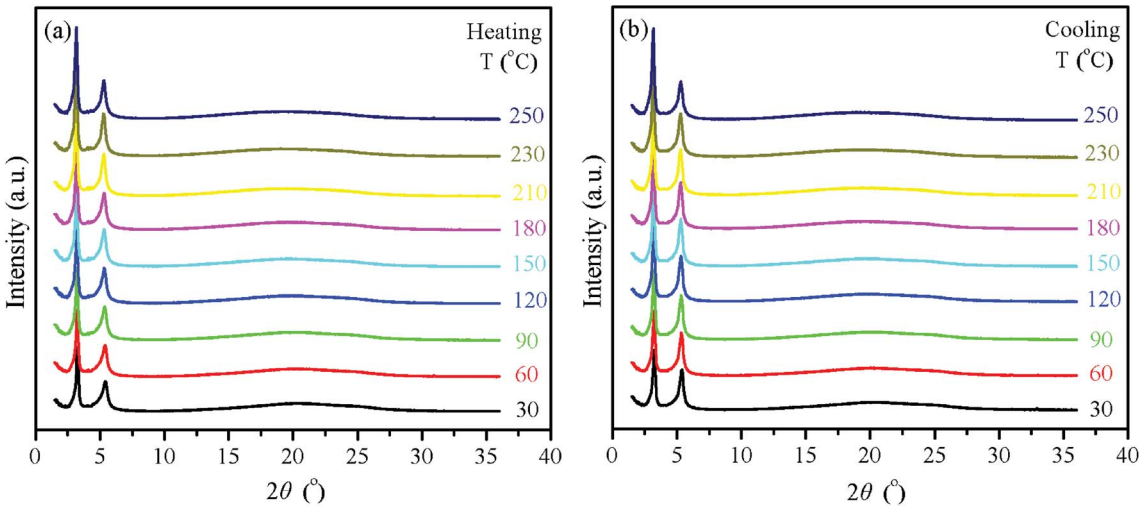

Fig. 7 1D WAXD patterns of PBTCS during the first heating (a) and subsequent cooling (b).

By simulated calculation, the length of the Tp moiety with all-trans conformation of C6 alkyl arms is *ca.* 2.3 nm. Nevertheless, the whole side chain length cannot be precisely estimated, owing to the possible rotation of the ester linkage. However, depending on the relative position of Tp moieties in the side chain, the dimension of the whole side chain should be not exceeding 4.6 nm. Meantime, in the high-angle region, the broad weak peak at 2θ of ~25° indicates that there only exhibits weak π–π interactions of the side-chain triphenylene discogens (see Fig. 7a). Therefore, we presume that the structure of the LC phase is a hexagonal columnar (Φ_H) phase,[41,42] developed by the "jacketing effect" rod-like supramolecular mesogen, suggesting the mesogenic groups and main chain construct cylinders and the mesogenic groups were tilted ~45° away from the long axis of the cylinder.[43,44]

The 1D WAXD profiles in the heating process follow almost the same pathways as those in the cooling process. Fig. 8 shows plots of the *d*-spacing of the (100) diffraction (d_{100}) against temperature. A continuous increase of d_{100} is observed during heating with no transition, as the same cannot be detected in DSC. Upon cooling, a same continuous *d*-spacing decrease compared with that in the heating process, indicating the formation of the stable LC phase. Regardless of the heating process or the cooling process, the degree of order of this phase does not change much (2.72 nm to 2.80 nm).

In order to further elucidate the phase structure of PBTCS, we performed 1D SAXS experiment. The polymer was heated to 250 °C, and then slowly cooled to room temperature. Fig. 9 shows the 1D SAXS profiles of PBTCS. As can be seen, a first-order sharp peak is centered at $q^* = 2.23$ nm^{-1} and a secondary diffraction peak appears at $3^{1/2}q^* = 3.74$ nm^{-1}, and the ratio of $q^* : 3^{1/2}q^*$ was $1 : 3^{1/2}$, indicating a hexagonal columnar structure with a periodicity of 2.81 nm ($d_{100} = 2\pi/q^*$), which is consistent with the 1D WAXD results (2.74 nm).

2D WAXD experiments were carried out to further characterize the mesomorphic phase structure of PBTCS. Fig. 10a depicts the 2D WAXD pattern of PBTCS at room temperature. The film

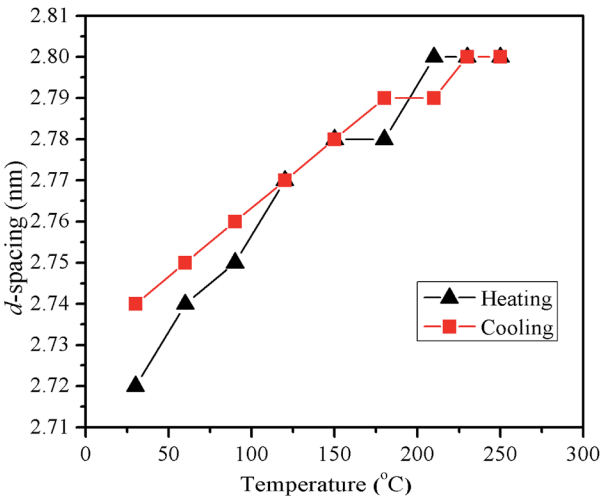

Fig. 8 *d*-Spacing values of the first diffraction peak in the 1D WAXD patterns of PBTCS during the first heating and subsequent cooling processes as a function of temperature.

sample was obtained and treated with a relatively large shear force at 250 °C. As can be noticed from the figure, with the shear direction on the meridian, two pairs of sharp arcs appear on the equator, indicating the existence of ordered structures on the nanometer scale with lattice planes oriented primarily parallel to the meridian direction. In general, the polymer chain will be oriented parallel to the direction of the shear force. Hence, the absence of the diffractions on other directions except those on the equator in the low-angle region ensured that all of the low-angle diffractions can be attributed to (*hk*0) diffractions. In particular, when setting the sample vertically and letting the X-ray beam go through *x*, 6-fold symmetry of the (110) diffractions can be observed, as shown in Fig. 10c, which elucidates more clearly the hexagonal packing, the corresponding azimuthal intensity profiles of six peaks were 31°, 91°, 152°, 214°, 274° and 335° (as shown in Fig. 10d). This observation is consistent with the

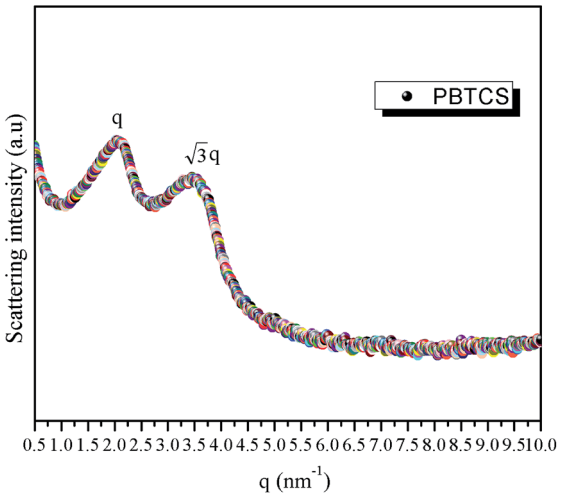

Fig. 9 1D SAXS profiles of PBTCS recorded at room temperature with intensity in log scale.

assignment of the diffraction peaks in 1D WAXD patterns. Therefore, all Tp moieties are aligned with the polymer main chain to form a stabilized ordered phase. Therefore, the 2D WAXD patterns combining the results of POM and 1D WAXD support that PBTCS possesses a 2D Φ_H phase developed by the rod-like supramolecular mesogen and main chain.

In order to certify the orientation of PBTCS, the sample was heated and oriented by shearing at 250 °C, and then slowly cooled to room temperature, and at last performed by POM. As shown in Fig. 11a, after the sample was oriented by shearing, the color of the texture was not bright enough; however, when the sample was rotated to an angle of ~45°, the color of the texture evidently changed (Fig. 11b), illustrating that the side chain Tp was perpendicular to the main chain, indicated that the orientation of the main chain was the same as the orientation of the shearing direction.[45]

The reconstructed relative electron density map of PBTCS was shown in Fig. 12. It is reasonable to assign the blue colored zone with low electron density to the alkyl tails of the triphenylene, the red colored zone with high electron density to the triphenylene discotic mesogens, while the core (orange colored) of the column with intermediate electron density around the red zones to the rigid backbones. The diameter of the columns in the reconstructed electron density map agreed well with the observed results by WAXD.

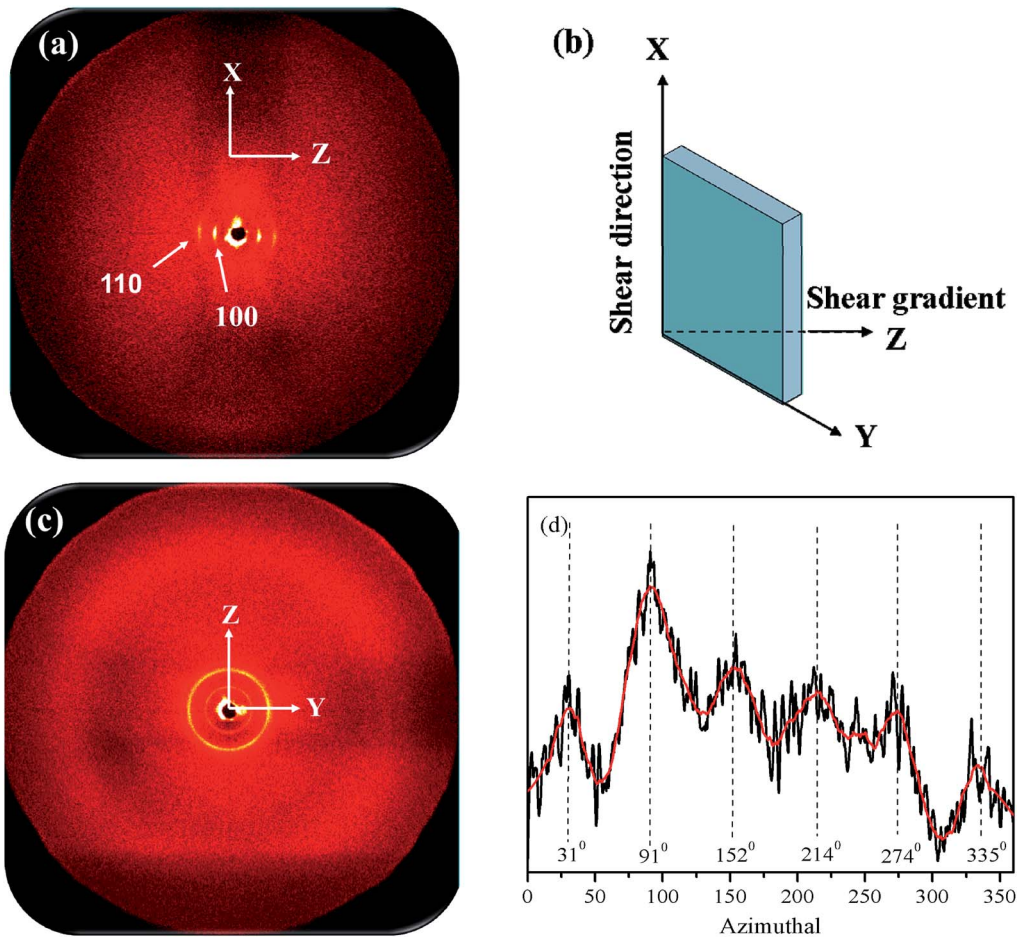

Fig. 10 2D WAXD patterns of PBTCS at room temperature, with the X-ray beam perpendicular (a) and parallel (c) to the shear direction, and the shearing geometry (b), where *X* and *Z* are the shear direction and shear gradient. The azimuthal scanning corresponds to the equator and the meridian (d).

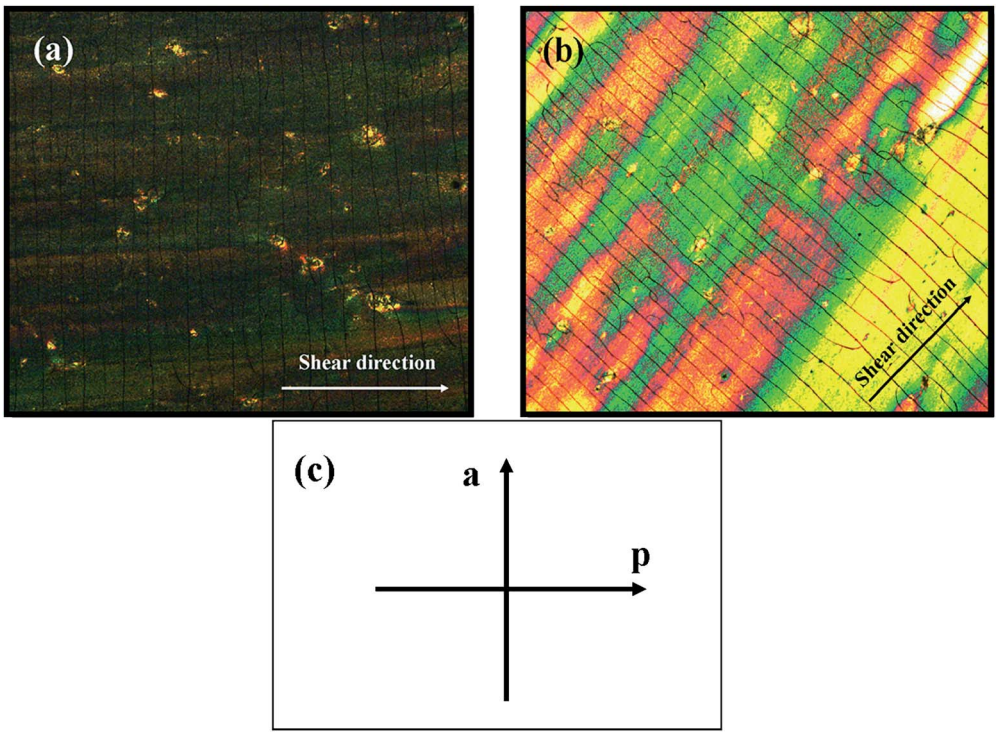

Fig. 11 Polarizing optical microscopy images of PBTCS prepared as follows: sheared at 250 °C (a and b). The arrows of *a* and *p* denote the directions of the analyzer and polarizer, respectively (c).

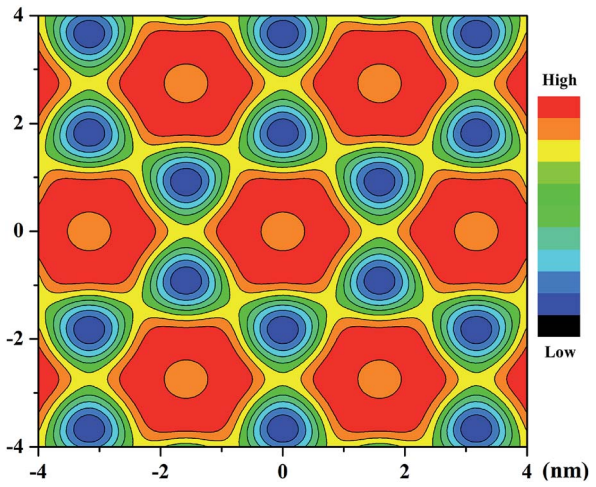

Fig. 12 The reconstructed relative electron density map of the 2D hexagonal lattice of PBTCS.

Fig. 13 depicts a schematic drawing of the molecular packing of PBTCS. From the entire test, we found that PBTCS exhibits a stabilized phase structure, and without flexible spacer between main chain and Tp moieties in the side chains, offers a stronger coupling effect, leading to overcoming the π–π interaction of Tp mesogen. As expected, without a flexible spacer, the T_g of PBTCS is 222 °C, which is higher than that of PP*n*V,[36,37] owing to the stronger steric hindrance. Meantime, PBTCS exhibited a stabilized hexagonal columnar (Φ_H) phase, whether at low or high temperature, which is different from the phase behavior of PP*n*V. At low temperatures, for PP3V and PP6V, both polymers formed rectangular columnar (Φ_R) phases in conjunction with a discotic nematic (N_D) phase, owing to the self-organization of the Tp moieties. For PP12V, it presented a hexagonal columnar (Φ_H) phase owing to the strong decoupling and was self-organized by Tp discotic mesogens. At high temperature, PP6V formed a Φ_H phase and PP12V formed a Φ_N phase developed by the rod-like supramolecular mesogen – the MJLCP chain as a whole. Compared with PBTCS, PP3V and PP6V, the Tp mesogen of PP12V showed a more ordered structure, suggesting that longer flexible spacers between MJLCP main chain and Tp moieties in the side chains offered a stronger decoupling effect, which allowed the two LC building blocks to act more independently. This result can be supported by the intensity of π–π stacking of the Tp.

The spacer length affects the interplay between the two LC building blocks tremendously. Without the spacer, two Tp mesogens were built like one calamitic mesogen only; therefore, the phase behavior is similar to many other MJLCPs.[39,40] By simulated calculation, the length of two Tp moieties with all-trans conformation of C6 alkyl arms is *ca.* 4.6 nm. Moreover, based on experimental results, the PBTCS formed the Φ_H phase ($a = b = 3.17$ nm) developed by the mesogen and main chain indicating that the mesogenic groups were tilted ~45° away from the long axis of the cylinder. For PP6V, it also formed a Φ_H phase ($a = b = 4.35$ nm) at the high temperature. But, the later polymers contained larger *a* and *b* values compared with PBTCS, due to the increased spacer length from zero methylene units to six. For PP12V, the Tp discotic mesogens can self-organize into the Φ_H phase ($a = b = 2.06$ nm), owing to the

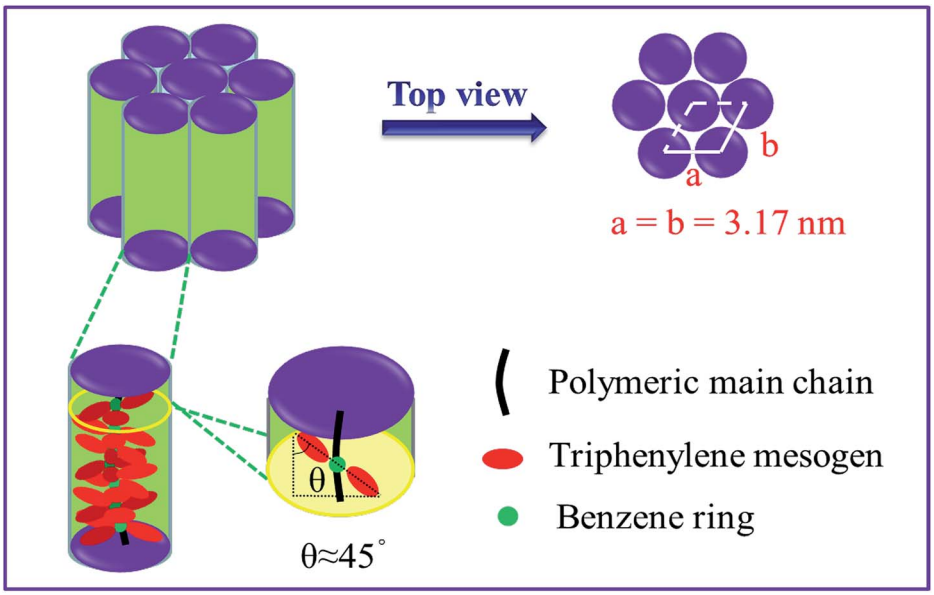

Fig. 13 Schematic drawing of the PBTCS.

strong decoupling. In simulated calculation, the length of the Tp moiety with all-trans conformation of C6 alkyl arms is *ca.* 2.3 nm, indicating the molecular plane of PP12V is nearly perpendicular to the formed column axis. Therefore, the spacer length plays a very important role in the arrangement of Tp side-chain mesogens in the MJLCPs system.

Conclusions

In summary, using conventional free radical polymerization, we synthesized a novel MJLCP bearing Tp DLCs as pendant groups, PBTCS, with sufficiently high M_w (M_n = 1.7 × 10^4 g mol^{-1}) to construct MJLCP with DLCs as the side-chain LC functional material. Combining 1D/2D WAXD and 1D SAXS results with POM and DSC observations, PBTCS exhibits a stabilized 2D Φ_H phase. As expected, when the flexible spacer is abolished, the "jacketing effect" is increased, leading to overcoming the π–π interaction of Tp mesogen. On the basis of our work, new functional materials with fine-tunable ordered structures can be provided, which is of great importance for both fundamental research and real applications.

Acknowledgements

This research was financially supported by the National Nature Science Foundation of China (51373148), and the Innovation Platform Open Foundation of University of Hunan Province (CX2013B265). The authors thank Prof. Chen Er-Qiang of Peking University for their help with 1D SAXS experiments measurements.

Notes and references

1 Z. Danli, T. D. Ibtissam, X. Yiming, K. Farid, K. Navaphun, B. Martin, G. Daniel, H. Benoît, D. Bertrand, A. I. Dimitri, L. Emmanuelle, K. David, M. Fabrice and A. André-Jean, *Macromolecules*, 2014, **47**, 1715–1731.
2 M. W. C. P. Franse, K. Te Nijenhuis and S. J. Picken, *Rheol. Acta*, 2003, **42**, 443–453.
3 S. K. Pal and S. Kumar, *Liq. Cryst.*, 2008, **35**, 381–384.
4 K. Sandeep and K. V. Sanjay, *Org. Lett.*, 2002, **4**, 157–159.
5 M. T. Allen, S. Diele, K. D. M. Harris, T. Hegmann, B. M. Kariuki, D. Lose, J. A. Preece and C. Tschierske, *J. Mater. Chem.*, 2001, **11**, 302–311.
6 S. Kumar, *Chem. Soc. Rev.*, 2006, **35**, 83–109.
7 R. I. Gearba, D. V. Anokhin, A. I. Bondar, W. Bras, M. Jahr, M. Lehmann and D. A. Ivanov, *Adv. Mater.*, 2007, **19**, 815.
8 S. Sergeyev, W. Pisula and Y. H. Geerts, *Chem. Soc. Rev.*, 2007, **36**, 1902–1929.
9 U. Scherf, A. Gutacker and N. Koenen, *Acc. Chem. Res.*, 2008, **41**, 1086–1097.
10 P. H. J. Kouwer, W. F. Jager, W. J. Mijs and S. J. Picken, *J. Mater. Chem.*, 2003, **13**, 458–469.
11 X. Chen, L. Chen, K. Yao and Y. Chen, *ACS Appl. Mater. Interfaces*, 2013, **5**, 8321–8328.
12 H. K. Bisoyi and S. Kumar, *J. Mater. Chem.*, 2008, **18**, 3032–3039.
13 T. Emiliano, C. Rubeń, S. E. Gerardo, L. F. Ceśar, O. Josu, C. Silverio and E. Pablo, *Inorg. Chem.*, 2014, **53**, 3449–3455.
14 I. Julien, M. Raphael, D. Laurent, C. Freďeŕic, B. Harald, O. Yoann, C. Jeŕome, B. David, D. 'A. Gabriele, M. R. Otello, M. Luca and Z. Claudio, *J. Am. Chem. Soc.*, 2014, **136**, 2911–2920.
15 B. Wu, B. Mu, S. Wang, J. Duan, J. Fang, R. Cheng and D. Chen, *Macromolecules*, 2013, **46**, 2916–2929.
16 W. Kreuder and H. Ringsdorf, *Makromol. Chem., Rapid Commun.*, 1983, **4**, 807–815.
17 C. M. Xing, J. W. Y. Lam, K. Q. Zhao and B. Z. Tang, *J. Polym. Sci., Part A: Polym. Chem.*, 2008, **46**, 2960–2974.

18 I. Tahar-Djebbar, F. Nekelson, B. Heinrich, B. Donnio, D. Guillon, D. Kreher, F. Mathevet and A. J. Attias, *Chem. Mater.*, 2011, **23**, 4653–4656.
19 Z. Q. Yu, W. Y. L. Jacky, Z. Keqing, C. Z. Zhu, S. Yang, J. S. Lin, B. S. Li, J. H. Liu, E. Q. Chen and B. Z. Tang, *Polym. Chem.*, 2013, **4**, 996–1005.
20 Z. Q. Yu, W. Y. L. Jacky, C. Z. Zhu, E. Q. Chen and B. Z. Tang, *Macromolecules*, 2013, **46**, 588–596.
21 B. Hüser and H. W. Spiess, *Macromol. Rapid Commun.*, 1988, **9**, 337–343.
22 B. Hüser, T. Pakula and H. W. Spiess, *Macromolecules*, 1989, **22**, 1960–1963.
23 H. Ringsdorf, R. Wüstefeld, E. Zerta, M. Ebert and J. H. Wendorff, *Angew. Chem., Int. Ed.*, 1989, **28**, 914–918.
24 M. Werth and H. W. Spiess, *Macromol. Rapid Commun.*, 1993, **14**, 329–338.
25 N. Boden, R. J. Bushby and Z. B. Lu, *Liq. Cryst.*, 1998, **25**, 47–58.
26 C. T. Imrie, R. T. Inkster, Z. Lu and M. D. Ingram, *Mol. Cryst. Liq. Cryst.*, 2004, **408**, 33–43.
27 D. Stewart, G. S. Mchattie and C. T. Imrie, *J. Mater. Chem.*, 1998, **8**, 47–51.
28 D. Zhang, Y. X. Liu, X. H. Wan and Q. F. Zhou, *Macromolecules*, 1999, **32**, 5183–5185.
29 C. Ye, H. L. Zhang, Y. Huang, E. Q. Chen, Y. L. Lu, D. Y. Shen, *et al.*, *Macromolecules*, 2004, **37**, 7188–7196.
30 X. Z. Wang, H. L. Zhang, E. Q. Chen, X. Y. Wang and Q. F. Zhou, *J. Polym. Sci., Part A: Polym. Chem.*, 2005, **43**, 3232–3244.
31 H. L. Xie, T. H. Hu, X. F. Zhang, H. L. Zhang, E. Q. Chen and Q. F. Zhou, *J. Polym. Sci., Part A: Polym. Chem.*, 2008, **46**, 7310–7320.
32 Y. Guan, X. F. Chen, Z. H. Shen, X. H. Wan and Q. F. Zhou, *Polymer*, 2009, **50**, 936–944.
33 Y. D. Xu, Q. Yang, Z. H. Shen, X. F. Chen, X. H. Fan and Q. F. Zhou, *Macromolecules*, 2009, **42**, 2542–2550.
34 L. Y. Zhang, Z. H. Shen, X. H. Fan and Q. F. Zhou, *J. Polym. Sci., Part A: Polym. Chem.*, 2011, **49**, 3207–3217.
35 Y. X. Liu, D. Zhang, X. H. Wan and Q. F. Zhou, *Chin. J. Polym. Sci.*, 1998, **16**, 283–288.
36 Y. F. Zhu, X. L. Guan, Z. H. Shen, X. H. Fan and Q. F. Zhou, *Macromolecules*, 2012, **45**, 3346–3355.
37 Y. F. Zhu, H. J. Tian, H. W. Wu, D. Z. Hao, Y. Zhou, Z. H. Shen, D. C. Zou, P. C. Sun, X. H. Fan and Q. F. Zhou, *J. Polym. Sci., Part A: Polym. Chem.*, 2014, **52**, 295–304.
38 H. Ringsdorf, P. Tschirner, O. H. Schonherr and J. H. Wendorff, *Makromol. Chem.*, 1987, **188**, 1431–1445.
39 X. F. Chen, Z. Shen, X. H. Wan, X. H. Fan, E. Q. Chen, Y. Ma and Q. F. Zhou, *Chem. Soc. Rev.*, 2010, **39**, 3072–3101.
40 H. L. Xie, S. J. Wang, G. Q. Zhong, Y. X. Liu, H. L. Zhang and E. Q. Chen, *Macromolecules*, 2011, **44**, 7600–7609.
41 V. Percec, T. K. Bera, M. Glodde, Q. Fu, V. S. K. Balagurusamy and P. A. Heiney, *Chem. - Eur. J.*, 2003, **9**, 921.
42 V. Percec, M. R. Imam, M. Peterca and P. Leowanawat, *J. Am. Chem. Soc.*, 2012, **134**, 4408.
43 C. Ye, H. L. Zhang, Y. Huang, E. Q. Chen, Y. L. Lu, Y. L. Shen, X. H. Wan, Z. H. Shen, S. Z. D. Cheng and Q. F. Zhou, *Macromolecules*, 2004, **37**, 7188–7196.
44 C. Y. Li, K. K. Tenneti, D. Zhang, H. Zhang, X. Wan, E. Q. Chen, Q. F. Zhou, A. O. Carlos, S. Igos and B. S. Hsiao, *Macromolecules*, 2004, **37**, 2854–2860.
45 L. Y. Zhang, Z. H. Shen, X. H. Fan and Q. F. Zhou, *J. Polym. Sci., Part A: Polym. Chem.*, 2011, **49**, 3207–3217.